*36th EPS Conference on Plasma Phys. Sofia, June 29 - July 3, 2009 ECA Vol.**33E**, P-2.038 (2009)*

Integrated Simulations of Core Heating in FIREX-I

T. Johzaki[1], H. Nagatomo[1], A. Sunahara[2], H. Sakagami[3], Y. Nakao[4], and K. Mima[1]

[1]*Institute of Laser Engineering, Osaka University, Osaka, Japan*

[2]*Institute for Laser Technology, Osaka, Japan*

[3]*Department of Simulation Science, National Institute for Fusion Science, Toki, Japan*

[4]*Department of Applied Quantum Physics and Nuclear Engineering, Kyushu University, Fukuoka, Japan*

1. INTRODUCTION

In the cone-guiding fast ignition, an imploded core is heated by the energy transport of fast electrons generated by the ultra-intense short-pulse laser at the cone inner surface. The fast core heating (~800eV) has been demonstrated at integrated experiments with GEKKO-XII+ PW laser systems [1]. As the next step, experiments using more powerful heating laser [Fast Ignition Realization Experiment (FIREX) at ILE Osaka university [2] and OMEGA-EP at LLE university of Rochester [3]] have been started. In FIREX-I (phase-I of FIREX), our goal is the demonstration of efficient core heating (T_i ~ 5keV) using a newly developed 10kJ/10ps LFEX laser. In the first integrated experiments in FIREX-I, the LFEX laser is operated with low energy mode (~0.5kJ/4ps) to validate the previous GEKKO+PW experiments. Between the two experiments, though the laser energy is similar (~0.5kJ), the duration is different; ~0.5ps in the PW laser and ~ 4ps in the LFEX laser. In this paper, we evaluate the dependence of core heating properties on the heating pulse duration on the basis of integrated simulations with FI^3 (Fast Ignition Integrated Interconnecting) code system [4-9].

2. SIMULATION CONDITION

The FI^3 code consists of four codes; an ALE Radiation-hydro code “PINOCO,” a one-dimensional (1D) radiation hydro code “Star-1D”, a collective PIC code “FISCOF” and a coupled relativistic Fokker-Planck (RFP) and hydro code “FIBMET”. The procedure of core heating simulation is as follows. First, we carry out implosion simulations for an Au cone attached CD shell target using PINOCO to obtain the compressed core profile. For heating phase, low-density brow-off plasma on the cone-inner surface produced by the pre-pulse of heating laser, that is pre-plasma, is evaluated by a radiation-hydro code Star1D. Using the pre-plasma profile, the time-dependent fast electron profile is evaluated using FISCOF. The following energy transport into the imploded dense core is simulated by FIBMET where the time-dependent fast electron profile evaluated by FISCOF simulation is used as the external fast electron source, and the imploded core profile obtained by PINOCO simulation is used as the initial condition of bulk plasma. In the core heating, the multidimensional natures are of course important. However, full scale (time and space) multidimensional simulations are very expensive. Thus, for the present study, we used 1D version of PIC and RFP-hydro codes.

3. SIMULATION RESULTS

3.1 Fast Electron Generation

For evaluation of fast electron profiles, we carried out 1D PIC simulations where electros

and ions (Au, Z=50) are mobile and the collision process is not included. The cone tip is modeled by $500n_c$ and 10μm thickness plasma. The pre-plasma generated by the pre-pulse of heating laser is attached on the laser irradiated surface. In the present study, we assumed the 3 different scale lengths for the pre-plasma, "short", "middle" and "long" (see **Fig,1**), on the basis of star-1D radiation-hydro simulations by assuming different pre-pulse intensities. On the rear surface of the cone tip, we located 20μm thickness imploded CD plasma with n_e = 500n_c. The generated fast electron profile is observed in the CD plasma region. The heating laser is the Gaussian pulse with λ_L = 1.06μm. The pulse duration and intensity are (a) τ_{FWHM} = 0.5ps and I_L = 7.03x10^{19}W/cm^2 (PW case) and (b) τ_{FWHM} = 4ps and I_L = 0.88x10^{19}W/cm^2 (LFEX case). The irradiated laser energy is 0.37J/μm^2, which corresponds to 500J when the laser spot diameter is 40μm.

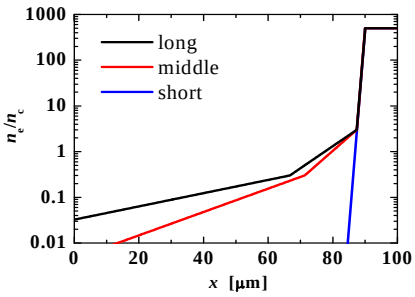

Fig.1 Spatial profiles of pre-plasma for 3 cases

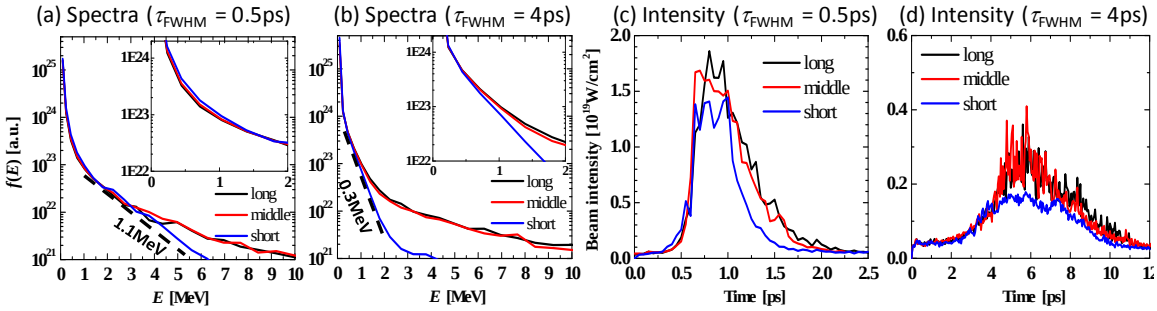

Fig.2 Fast electron profiles; time-integrated energy spectra for (a) τ_{FWHM} = 0.5ps and (b) τ_{FWHM} = 4.0ps, and temporal profiles of beam intensity for (c) τ_{FWHM} = 0.5ps and (d) τ_{FWHM} = 4.0ps.

In **Fig.2**, we show the observed fast electron profiles; time-integrated energy spectra and temporal profiles of beam intensity for 3 different scale-length cases with 2 different laser durations. The beam intensity of fast electron and its slope temperature in the relatively low energy region are higher in the short pulse case (τ_{FHWM} = 0.5ps) since the intensity is higher.

In the short scale length case, the fast electron slope temperature evaluated from time-integrated spectra are 1.1MeV for τ_{FHWM} = 0.5ps and 0.3MeV for τ_{FHWM} = 4ps. However, the laser intensity changes with time, so that the temperature of generated fast electron also changes with time. In **Fig.3**, we plotted the fast electron temperature T_h evaluated from the spectra observed at the

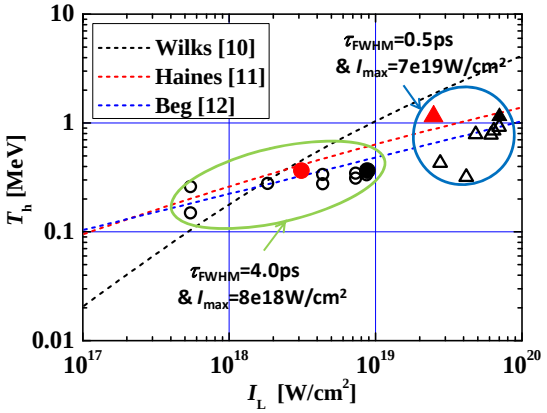

Fig.3 Fast electron temperature as a function of laser intensity. The circles (triangles) indicates Th for the case of τ_{FWHM} = 4.0ps (0.5ps). Open marks represent T_h evaluated from the spectra observed at the different times during the simulations and solid marks T_h evaluated from time-integrated spectra. Red solid marks are plotted as a function of peak laser intensity and black solid marks as a function of time-averaged laser intensity.

different times (open marks), and T_h evaluated from the time integrated spectra (solid marks) for short scale-length case as a function of laser intensity, together with the scaling law [10-12]. The dependence of T_h on laser intensity is close to Beg's and Haines's scaling, rather than Wilks's scaling.

On the other hand, in the middle and long scale-length cases, the electron spectra have high-energy tails, of which electrons are generated at the laser-plasma interaction in the under-dense region. Due to these high-energy tails, the beam intensity is higher in the middle and long scale-length cases compared to the short scale-length case. In FIREX-I, the implosion laser energy is low (several kJ), so the core size is not so large (ρR obtained in the present implosion simulation is 0.12g/cm^2). Thus the energetic fast electrons (*e.g.*, E > 2MeV) can hardly contribute to core heating; the core is mainly heated by relatively low energy fast electron (E < 2MeV). In Fig.2(a) and (b), the spectra in the energy range of E < 2MeV are enlarged. For τ_{FHWM} = 0.5ps, the difference of the energy spectrum in low energy region among 3 different scale-length cases are small (slightly higher in the short scale case). For τ_{FHWM} = 4.0ps, however, T_h in the short scale case is too low (T_h = 0.3MeV). The high-energy tails in the middle and long scale cases hence enhance the number of electrons in the energy range of E > 0.5MeV. The fast electron beam energies are summarized in **Table I**. The energy coupling of heating laser to fast electron is low (20~ 40%) because of lack of multi-dimensional effects.

Table I Fast electron beam energy

τ_{FWHM}	0.5ps			4.0ps		
Scale length	**Short**	**Middle**	**Long**	**Short**	**Middle**	**Long**
Total [J/μm²] (coupling (%))	**0.089** (23.9)	**0.119** (31.8)	**0.125** (33.6)	**0.105** (28.0)	**0.143** (38.2)	**0.144** (38.4)
0 ~ 0.3MeV (coupling (%))	**0.0378** (10.1)	**0.0349** (9.0)	**0.0331** (8.9)	**0.0795** (21.3)	**0.0641** (17.2)	**0.0581** (15.6)
0.3~2MeV (coupling (%))	**0.0274** (7.3)	**0.0244** (6.5)	**0.0235** (6.3)	**0.020** (5.4)	**0.0264** (7.0)	**0.0280** (7.5)
2MeV ~ (coupling (%))	**0.0243** (6.5)	**0.0611** (16.3)	**0.0688** (18.4)	**0.0032** (1.4)	**0.0523** (14.0)	**0.0570** (15.3)

The values in () are the energy coupling of heating laser to fast electron.

3.2 Core Heating

Using the time-dependent profiles of fast electron, we carried out the core heating simulations using 1D FIBMET. As for the bulk plasma profile, we use the imploded core profile at the central axis (**Fig.4**) obtained by 2D implosion simulation. The fast electrons are injected into the cone tip.

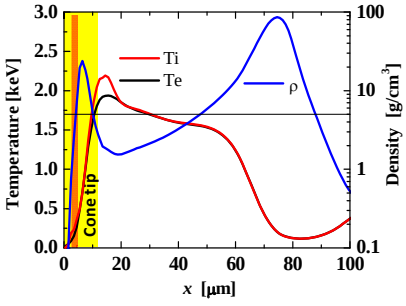

Fig.4 Imploded core profile at the central axis obtained by 2D implosion simulation. Yellow hatch indicates the cone tip region, fast electron injection points are indicated by orange hatch.

The results of core heating simulations are shown in **Fig.5**. The rise of ion temperature of dense core due to fast electron heating is 0.07keV ~ 0.1keV. These values are lower than that obtained in the previous experiments [1]. This is mainly due to the low energy coupling of heating laser to fast electron in the 1D PIC simulations. The difference in rise of core temperature due to the pulse duration is not significant. The dependence on the pre-plasma scale length, however, differs between the short and long pulse cases. For τ_{FWHM} = 0.5ps, the low energy component of fast electron (E < 2.0MeV) slightly higher in the short scale case, so that the rise of core temperature is higher compared to the middle and long scale cases. On the other hand, for τ_{FWHM} = 4.0ps, since the slope temperature of fast electron is too low in the short scale case, the low energy component of fast electron is larger in the middle

and long scale cases. Thus the rise of core temperature is higher in the middle and long scale cases. The similar dependences of core heating properties on pre-plasma scale length were obtained in our previous works for the short [13] and long [14] duration cases. It should be noted that the energy deposition of fast electron in the cone region is higher than that in the core region, especially for the long pulse case. The energy loss in the cone region lowers the core heating efficiency. To reduce this energy loss, we had proposed use of low-Z materials as an alternative of cone tip [15].

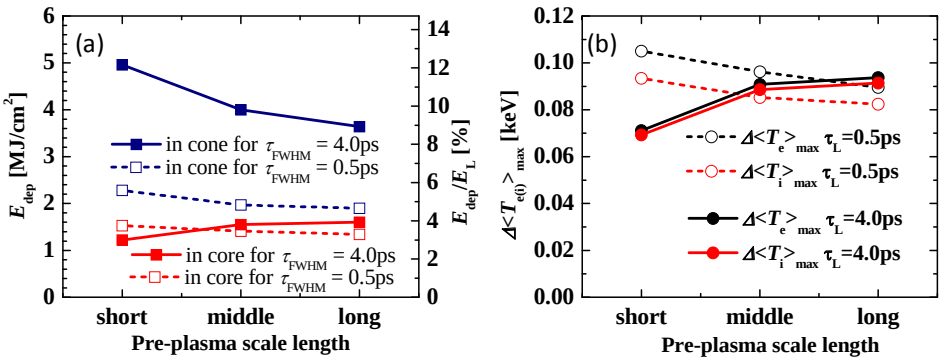

Fig.5 (a) deposited energy of fast electrons in cone and core (ρ > 5g/cm^3) regions and (b) rises of mass-averaged core temperatures $\Delta<T_{e(i)}>_{max}$ for τ_{FHWM} = 0.5ps and 4.0ps cases as a function of pre-plasma scale length. $\Delta<T_{e(i)}>_{max}$ is defined as $<T_{e(i)}>_{max} - <T_{e(i)}>(0)$, where $<T_{e(i)}>_{max}$ and $<T_{e(i)}>(0)$ are the maximum and initial values of mass-averaged electron (ion) temperature in the core region.

4. CONCULUDING REMARKS

It was found from the 1D integrated simulations that the difference in the core heating efficiency due to the heating laser pulse duration is not significant when the heating laser energy is low (here ~500J for 40μm spot diameter). For more realistic evaluation, the multi-dimensional study is in progress.

ACKNOWLEDGMENTS

This work was supported by MEXT, Grant-in-Aid for Scientific Research (C) (20540482) and (19540528), JSPS, Core-to-Core Program (19003), and Photon Pioneers Center in Osaka University.

REFERENCES

[1] R. Kodama et al., Nature, **412**, 798 (2001); ibid., **418**, (2002) 933.
[2] H. Azechi and the FIREX Project, Plasma Phys. Control. Fusion **48**, (2006) B267.
[3] C. Stoeckl, et al., Fusion Sci. Technol. **49**, (2006) 367.
[4] H. Nagatomo, et al., Proc. 2nd IFSA, Kyoto, Japan, (Paris: Elsevier) (2001) 140.
[5] A. Sunahara, at al., Plasma Fusion Res. **3** (2008) 043.
[6] H. Sakagami and K. Mima, Laser Part. Beams **22**, (2004) 41.
[7] H, Sakagami, et al., Laser Part. Beams **24**, (2006) 191.
[8] T. Yokota, et al., Phys. Plasmas **13**, (2006) 022702.
[9] T. Johzaki, et al., J. Plasma Res. SERIES 6 (2004)341.
[10] S. C. Wilks, et al., Phys. Rev. Lett. **69**, (1992) 1383.
[11] F. N. Beg, et al., Phys. Plasmas **4**, (1997) 447.
[12] M. G. Haines, et al., Phys. Rev. Lett. **12**, (2009) 045008.
[13] T. Johzaki, et al., Laser Part. Beams **25**, (2007) 621.
[14] H. Sakagami, et al., J. Phys.: Conf. Series **112** (2008) 022070.
[15] T. Johzaki, et al., Plasma Phys. Control. Fusion **51**, (2009) 014002.